

Rotational velocities of the giants in symbiotic stars: II. Are S-type symbiotics synchronized? ^{*}

R. K. Zamanov^{1,2} †, M. F. Bode², C. H. F. Melo^{3,4}, R. Bachev¹,
A. Gomboc^{2,5}, I. K. Stateva¹, J. M. Porter², J. Pritchard³

¹ *Institute of Astronomy, Bulgarian Academy of Sciences, 72 Tsarigradsko Shousse Blvd., 1784 Sofia, Bulgaria*

² *Astrophysics Research Institute, Liverpool John Moores University, Twelve Quays House, Birkenhead, CH41 1LD, UK*

³ *European Southern Observatory, Casilla 19001, Santiago 19, Chile*

⁴ *Departamento de Astronomía, Universidad de Chile, Casilla 36-D, Santiago, Chile*

⁵ *Department of Physics, University of Ljubljana, Jadranska 19, 6100 Ljubljana, Slovenia*

Accepted . Received 2007 May 17; in original form 2006 March 17

ABSTRACT

We have measured the projected rotational velocities ($v \sin i$) of the mass donors for 29 S-type symbiotic stars using high resolution spectroscopic observations and the cross-correlation function (CCF) method. The results of the CCF have been controlled with synthetic spectra. The typical rotational velocity of the K and M giants in S-type symbiotics appeared to be $4.5 < v \sin i < 11.7 \text{ km s}^{-1}$. In a sub-sample of 16 S-type symbiotic stars (with known orbital periods and well measured $v \sin i$) 15 have deviations from synchronization less than the $3\text{-}\sigma$ level. This means that we did not find evidence for a statistically significant deviation from the synchronization for any of these 15 objects. The deviation from synchronization is statistically significant (at confidence level $>99\%$) only for the recurrent nova RS Oph.

For 22 S-type symbiotics we give clues as to what their orbital periods could be.

Key words: stars: binaries: symbiotic – stars: rotation – stars: late type

1 INTRODUCTION

The Symbiotic stars (SSs – thought to comprise a white dwarf (WD) accreting from a cool giant or Mira) represent the extremum of the interacting binary star classification. They offer a laboratory in which to study such important processes as (i) mass loss from cool giants and the formation of Planetary Nebulae; (ii) accretion onto compact objects, (iii) photoionisation and radiative transfer in gaseous nebulae, and (iv) nonrelativistic jets and bipolar outflows (e.g. Kenyon 1986; Corradi et al. 2003).

On the basis of their IR properties, SSs have been classified into stellar continuum (S) and dusty (D or D') types (Allen 1982). The D-type systems contain Mira variables as mass donors. The D'-type are characterized by an earlier spectral type (F-K) of the cool component and lower dust temperatures. All mass donors in D'-type systems appeared to be very fast rotators (see Paper I, Zamanov et al. 2006).

Our aims here are: (1) to measure the projected rota-

tional velocities ($v \sin i$) and the rotational periods (P_{rot}) of the giants in a number of southern S-type SSs, using a cross correlation function (CCF) approach; (2) to check whether their rotation is synchronized with the orbital period; (3) to provide pointers to the determination of binary periods (assuming co-rotation).

This is the second in a series of papers exploring the rotation velocities of the mass donating (cool) components of SSs.

2 OBSERVATIONS

We have observed 30 objects from the Belczyński et al. (2000) SS catalogue and have observed all S-type SSs from the catalogue with $12^h < RA < 24^h$, declination $< 2^0$, and catalogue magnitude brighter than $V < 12.5$.

The observations have been performed with FEROS at the 2.2m telescope (ESO, La Silla). FEROS is a fibre-fed echelle spectrograph, providing a high resolution of $\lambda/\Delta\lambda = 48000$, a wide wavelength coverage from about 4000 Å to 8900 Å in one exposure and a high throughput (Kaufer et al. 1999). The 39 orders of the echelle spectrum are registered with a $2k \times 4k$ EEV CCD

^{*} based on observations obtained in ESO programs 073.D-0724A and 074.D-0114

† e-mail: r kz@astro.bas.bg; mfb@astro.livjm.ac.uk; andreja.gomboc@mf.uni-lj.si

Table 1. Journal of observations. In the table are given as follows: the name of the object, date of observation (YYYY-MM-DD), the modified Julian Date (JD - 2400000.5) of the start of the observation, signal to noise ratio (S/N) around λ 8500 Å.

| object | date-obs | MJD-OBS | Exp [sec] | S/N |
|-------------|------------|------------|--------------|-----|
| AR Pav | 2004-06-04 | 53160.3737 | 600 | 40 |
| AS 255 | 2004-04-12 | 53107.3670 | 1200 | 45 |
| AS 276 | 2004-04-12 | 53107.3967 | 600 | 45 |
| AS 289 | 2004-06-05 | 53161.3071 | 600 | 40 |
| AS 316 | 2004-06-07 | 53163.3600 | 1200 | 70 |
| AS 327 | 2004-09-21 | 53269.0508 | 600 | 45 |
| BD-21°3873 | 2004-04-14 | 53109.2903 | 600 | 80 |
| CD-36°8436 | 2004-04-11 | 53106.3374 | 600 | 40 |
| CD-43°14304 | 2004-08-30 | 53247.2435 | 1200 | 70 |
| FG Ser | 2004-06-03 | 53159.2731 | 1200 | 50 |
| HD 319167 | 2004-06-07 | 53163.3905 | 600 | 45 |
| Hen 2-374 | 2004-06-08 | 53164.3099 | 1200 | 40 |
| Hen 3-1213 | 2004-04-12 | 53107.3049 | 1200 | 75 |
| Hen 3-1341 | 2004-04-12 | 53107.3354 | 1200 | 50 |
| Hen 3-1674 | 2004-06-07 | 53163.3103 | 1200 | 35 |
| Hen 3-1761 | 2004-06-04 | 53160.2095 | 600 | 40 |
| Hen 3-863 | 2004-04-11 | 53106.3067 | 1200 | 55 |
| MWC 960 | 2004-06-08 | 53164.2738 | 1200 | 70 |
| PN Ap 1-9 | 2004-06-07 | 53163.1986 | 1200 | 45 |
| RS Oph | 2004-04-11 | 53106.3849 | 600 | 50 |
| RW Hya | 2004-04-12 | 53107.2285 | 600 | 80 |
| SS73 129 | 2004-06-29 | 53185.0660 | 1200 | 65 |
| SS73 141 | 2004-06-29 | 53185.1058 | 1200 | 50 |
| V2506 Sgr | 2004-06-07 | 53163.2393 | 1200 | 45 |
| V2756 Sgr | 2004-06-08 | 53164.3968 | 600 | 40 |
| V2905 Sgr | 2004-06-28 | 53184.0858 | 1200 | 90 |
| V3804 Sgr | 2004-06-27 | 53183.9951 | 1200 | 40 |
| V4018 Sgr | 2004-08-31 | 53248.1800 | 1200 | 50 |
| V4074 Sgr | 2004-06-07 | 53163.2737 | 600 | 50 |
| V919 Sgr | 2004-06-03 | 53159.3108 | 1200 | 50 |

The present data have been collected from April to September 2004. Table 1 gives a log of the observations. All spectra are reduced using the dedicated FEROS data reduction software implemented in the ESO-MIDAS system (www.lis.eso.org/lasilla/sciops/2p2/E2p2M/FEROS/DRS/). A few examples of our spectra are given in the Appendix (Fig.4).

3 $v \sin i$ MEASUREMENT TECHNIQUES

3.1 CCF method

The projected rotational velocities have been derived by cross-correlating the observed spectra with K0 numerical masks yielding a cross-correlation function whose width (σ_{obs}) is related to broadening mechanisms such as stellar rotation and turbulence.

The emission lines do have an effect in the CCF and they must be cleaned. They were cut off by fitting a continuum and replacing the emission lines by the value of the fit. Note that the exact location of the continuum is not important.

The numerical K0-mask was constructed from a K0III

synthetic spectrum in the region between $\lambda\lambda$ 5000-7000 Å following the procedure described in Baranne et al. (1979) In the CORAVEL-type cross-correlation a binary mask is used as template instead a real spectrum. This binary (or CORAVEL-type) mask has been used in many different data reduction software for cross-correlation (ELODIE, CORALIE, and now HARPS). The K0-mask CCFs for the SSs observed here are plotted in the Appendix (Fig.5) and σ_{obs} are given in Table 2.

In order to use the observed width of the CCF (σ_{obs}) as an estimate of $v \sin i$ one needs to subtract the amount of broadening contributing to σ_{obs} unrelated to the stellar rotation (convection, instrumental profile, etc), i.e. σ_0 . For FEROS spectra (see Melo et al. 2001, 2003):

$$v \sin i = 1.9 \sqrt{\sigma_{obs}^2 - \sigma_0^2} \text{ km s}^{-1} \quad (1)$$

More details of the cross-correlation procedure are given in Melo et al. (2001), and also σ_0 is calibrated as a function of the $(B - V)$ for FEROS spectra and for stars with $0.6 < (B - V) < 1.2$. For giants with $(B - V) < 1.2$ in Table 2 as well as in Paper I, the Melo et al.(2001) calibration has been adopted. However, the stars in our sample have $(B - V)$ around 1.5 which is beyond the range of the calibration of Melo et al.(2001). For $(B - V) > 1.2$, we will adopt constant $\sigma_0 = 4.5 \text{ km s}^{-1}$.

This value has been adopted as a result of: **(i)** CCF measurements of few objects with known $v \sin i$; **(ii)** bearing in mind the results of Delfosse et al. (1998). Using a similar template and method but lower resolution (which increases σ_0), Delfosse et al. (1998) have shown that σ_0 does vary over a range of $0.8 < (R - I) < 1.5$ (which corresponds to a spectral type from $\sim M0$ to $\sim M6$), decreasing from $\sim 5.1 \text{ km s}^{-1}$ to 4.7 km s^{-1} ; **(iii)** bearing in mind the calibration of CCF and FEROS spectra undertaken in Melo et al. (2001).

The errors on CCF $v \sin i$ measurements are dominated by systematic effects rather than by photon noise. The error on $v \sin i$ comes from two main sources: uncertainties on the values of σ_{obs} and σ_0 . According to error estimate carried out by Melo et al.(2001), stars with $(B - V) < 1.2$ have an error on $v \sin i$ less than 1.2 km s^{-1} . For stars with $(B - V) > 1.2$ we adopt a constant σ_0 , which leads to an increase in our errors. For such stars a conservative error of 1.5 km s^{-1} is assigned. For objects with $v \sin i \geq 15 \text{ km s}^{-1}$ the error on $v \sin i$ is $\pm 10\%$.

In the case of the rapidly rotating Hen 3-1674 the CCF rotation was extracted by a slightly different procedure as described for the fast rotators in Paper I. For V3804 Sgr we did not get a meaningful CCF due to the numerous emission lines in the spectrum at the time of our observations. From measurements of the FeI 8689 line we obtain a rough estimate of FWHM(FeI 8689) $\approx 0.58 \pm 0.15 \text{ Å}$ similar to the width of this line in AR Pav and FG Ser and corresponding to $v \sin i \approx 9 \pm 3 \text{ km s}^{-1}$.

3.2 FWHM method

Besides the cross-correlation procedure another method using full width at half maximum (FWHM) of spectral lines of observed and synthetic spectra was also applied. This procedure is similar to that described in Fekel (1997). The spectra of K5III ($T_{eff}=3950 \text{ K}$, $\log g = 1.5$), M0III ($T_{eff}=3985$

Table 2. Rotational velocities of the red giants in symbiotic stars (measured in this paper). The spectral types are from the catalogue of Belczyński et al.(2000), (B-V)₀ is the intrinsic colour (from Schmidt-Kaler 1982) for the corresponding spectral type adopting luminosity class III in all cases, R_g is the adopted radius of the giant [if not otherwise indicated, this is the average radius for the corresponding spectral type taken from Table 7 of van Belle et al.(1999)]. P_{orb} is the orbital period (see Sect.6). $v \sin i$ (FWHM) is the projected rotational velocity of the cool giant as measured with FWHM method (see Sect.3.2). σ_{obs} is the observed width of the CCF. $v \sin i$ is our measurement based on CCF method (see Sect.3.1), if other measurements of $v \sin i$ exist, they are also given in the next column. For objects with unknown orbit we give an estimation of the upper limit of the orbital period P_{ul} (i.e. we expect P_{orb} ≲ P_{ul}, see Sect.9). The upper part of this table contains objects observed with FEROS, the lower part - $v \sin i$ values are taken from the literature.

| object | Cool | (B-V) ₀ | R _g | P _{orb} | $v \sin i$ FWHM | σ_{obs} CCF | $v \sin i$ CCF | other | P _{ul} |
|-------------|--------------|--------------------|----------------------|------------------|--------------------|-----------------------|-----------------------|---|-----------------|
| | Sp. | | R _☉ | [days] | km s ⁻¹ | [km s ⁻¹] | [km s ⁻¹] | [km s ⁻¹] | [days] |
| AR Pav | M5 | 1.59 | 139.6 | 604.5 | 8.8±2 | 6.208 | 8.1±1.5 | 11±2 ^e | — |
| AS 255 | K3 | 1.26 | 20.5 | | 9.7±1 | 6.417 | 8.7±1.5 | | 119 |
| AS 276 | M4.5 | 1.60 | 123.0 | | 7.7±2 | 6.382 | 8.6±1.5 | | 724 |
| AS 289 | M3.5 | 1.62 | 89.0 | 451 | 9.5±1 | 8.400 | 13.5±1.5 | 5.7±1 ^k | — |
| AS 316 | M4 | 1.62 | 105.5 | | 9.6±1 | 6.843 | 9.8±1.5 | | 545 |
| AS 327 | M3 | 1.62 | 71.5 | | 7.7±1 | 5.847 | 7.1±1.5 | | 510 |
| BD-21°3873 | K2 | 1.16 | 20.8 | 281.6 | 6.6±1 | 5.352 | 4.6±1.2 | 5.4±0.7 ^f | — |
| CD-36°8436 | M5.5 | 1.58 | 144.0 | | 6.6±1.5 | 6.410 | 8.7±1.5 | | 840 |
| CD-43°14304 | K5 | 1.51 | 38.8 | 1448 | 7.2±1 | 5.869 | 7.2±1.5 | <3 ^g | — |
| FG Ser | M5 | 1.59 | 139.6 | 650 | 9.8±1 | 6.756 | 9.6±1.5 | 8±1 ^h , 7±1 ^k | — |
| HD 319167 | M3 | 1.62 | 71.5 | | 7.4±2 | 6.041 | 7.7±1.5 | | 472 |
| Hen 2-374 | M5.5 | 1.59 | 144.0 | | 8.4±1.5 | 5.712 | 6.7±1.5 | | 1091 |
| Hen 3-1213 | M2/K4 | 1.54 | 50:? | | 9.1±1.5 | 7.236 | 10.8±1.5 | | 235 |
| Hen 3-1341 | M2 | 1.61 | 57.8 | | 7.5±1.5 | 6.423 | 8.7±1.5 | | 336 |
| Hen 3-1674 | M5 | 1.59 | 139.6 | | 56.0±5 | | 52.0±5.2 | | 135 |
| Hen 3-1761 | M4 | 1.62 | 105.5 | | 9.3±2 | 6.475 | 8.8±1.5 | | 603 |
| Hen 3-863 | K4 | 1.43 | 45.0 | | 7.9±1 | 5.811 | 7.0 ±1.5 | | 326 |
| MWC 960 | K9 | 1.55 | 39.0 ^a | | 9.0±1 | 6.436 | 8.7±1.5 | | 225 |
| PN Ap 1-9 | K4 | 1.43 | 45.0 | | 8.2±1 | 5.792 | 6.9±1.5 | | 329 |
| RS Oph | M0 | 1.56 | 59.1 | 455.7 | 13.8±1.5 | 7.624 | 11.7±1.5 | | — |
| RW Hya | M2 | 1.61 | 57.8 | 370.2 | 6.2±1 | 5.837 | 7.1±1.5 | 5.0±1 ^k | — |
| SS73 129 | M0 | 1.56 | 59.1 | | 8.9±1 | 6.162 | 8.0±1.5 | | 374 |
| SS73 141 | M5 | 1.59 | 139.6 | | 7.9±1 | 6.064 | 7.7±1.5 | | 914 |
| V2506 Sgr | M5.5 | 1.59 | 144.0 | | 7.8±1 | 6.284 | 8.3±1.5 | | 874 |
| V2756 Sgr | M3 | 1.62 | 71.5 | 243:? | 4.2±1.5 | 4.942 | 3.9±1.5 | | 932 |
| V2905 Sgr | M5 | 1.59 | 139.6 | | 6.6±1 | 5.708 | 6.7±1.5 | | 1059 |
| V3804 Sgr | M5 | 1.59 | 139.6 | | 9.0±3 | | | | ... |
| V4018 Sgr | M4 | 1.62 | 105.5 | | 7.2±1.5 | 5.345 | 5.5±1.5 | | 974 |
| V4074 Sgr | M4 | 1.62 | 105.5 | | 4.2±1.5 | 4.871 | 3.5±1.5 | | 1508 |
| V919 Sgr | M2 | 1.61 | 57.8 | | 7.4±1 | 6.560 | 9.1±1.5 | | 322 |
| SY Mus | M5 | | 139.6 | 624.5 | | | | 7±1 ^p | |
| AG Dra | K2Ib or II | | 30-40 ^b | 554 | | | | 3.6±1 ^k , 5.9±1 ^q | |
| BX Mon | M5III | | 139.6 | 1401 | | | | 6.8±1 ^k | |
| TX CVn | K5III | | 38.8 | 199 | | | | 8.9±1 ^k | |
| T CrB | M4IIIelips. | | 66±11 ^c | 227.57 | | | | 5.4±1 ^k | |
| V443 Her | M5.5III | | 144 | 594 | | | | 4.5±1 ^k | |
| CI Cyg | M5II or M5.5 | | 189-236 ^d | 854.5 | | | | 10.4±1 ^k | |
| AG Peg | M3III | | 71.5 | 817.4 | | | | 4.5±1 ^k | |
| V1329 Cyg | M6 | | 147.9 | 956.5 | | | | 7.0±2 ^k | |
| BF Cyg | M5III | | 75-280 ^r | 756.8 | | | | 4.5±2 ^k | |

^a-from the fit in van Belle et al.(1999); ^bTomov et al.(2000); ^cBelczynski & Mikolajewska(1998) ^dKenyon et al.(1995); ^eSchild et al.(2001); ^fSmith et al.(1997); ^gSchmid et al.(1998); ^hMürset et al.(2000); ^kFekel et al.(2003); ^pSchmutz et al.(1994); ^qde Medeiros & Mayor (1999). ^rsee Sect.6.2

K, $\log g = 1.2$), and M5III ($T_{eff}=3424$ K, $\log g = 0.5$), stars have been synthesized by using the code SYNSPEC (Hubeny, Lanz & Jeffery 1994) in the spectral region λ 8750-8850 Å.

LTE model atmospheres were extracted from Kurucz's

grid (1993). The VALD atomic line database (Kupka et al. 1999) was used to create a line list for spectrum synthesis. The value of 3 km s⁻¹ was adopted for the microturbulent velocity. A grid of synthetic spectra for projected rotational velocities from 0 km s⁻¹ to 60 km s⁻¹ was calculated. The

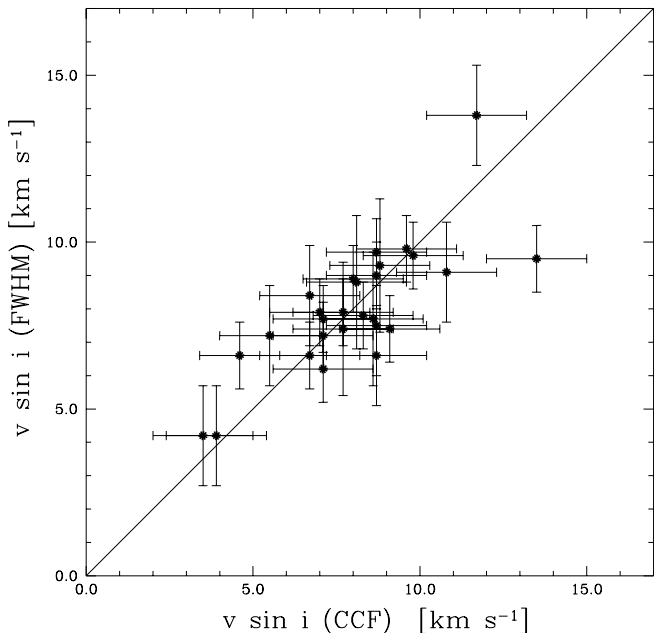


Figure 1. Comparison between the CCF and FWHM measurements of $v \sin i$. The straight line indicates $v \sin i(\text{CCF}) = v \sin i(\text{FWHM})$.

FWHM of a dozen observed spectral lines has been measured and compared to the FWHM of spectral lines from the synthetic spectra. The results are given in the sixth column of Table 2.

The comparison between the CCF and FWHM methods (see Fig.1) shows that the $v \sin i$ measurements agree well, with typical difference $\pm 1 - 2 \text{ km s}^{-1}$, as expected from the measurement errors. The only exception is AS 289 (see also Sect. 6.1).

Because the CCF method uses many more lines and a better defined mathematical procedure, in the analysis we will use $v \sin i$ derived with the CCF method.

4 PARAMETERS OF SYMBIOTIC STARS

4.1 Synchronization in SSs

The physics of tidal synchronization for stars with convective envelopes has been analyzed several times (e.g. Zahn 1977, and see the discussion in Chapter 8 of Tassoul 2000). There are some differences in the analysis of different authors, leading to varying synchronization timescales. Here, we use the estimate from Zahn (1977, 1989). The synchronization timescale in terms of the period is

$$\tau_{syn} \approx 800 \left(\frac{M_g R_g}{L_g} \right)^{1/3} \frac{M_g^2 \left(\frac{M_g}{M_2} + 1 \right)^2}{R_g^6} P_{orb}^4 \text{ years} \quad (2)$$

where M_g and M_2 are the masses of the giant and white dwarf respectively in Solar units, and R_g and L_g are the radius and luminosity of the giant, also in Solar units. The orbital period P_{orb} is measured in days.

In Table 3 we calculate this timescale for a few representative cases. We point out that these values serve as

Table 3. The synchronization time, τ_{syn} , calculated following Eq.1 for a few representative cases. The typical values for L_g and R_g of K5 III and M4III stars are adopted following van Belle et al.(1999).

| Mass donor Sp. type | L_g [L_\odot] | M_g [M_\odot] | R_g [R_\odot] | P_{orb} | M_2 [M_\odot] | τ_{syn} [yr] |
|------------------------|------------------------|------------------------|------------------------|-----------|------------------------|----------------------|
| K5 III | 350 | 2 | 40 | 200 d | 1.0 | 7000 |
| | | | | 1500 d | 1.0 | 2.10^7 |
| M4 III | 1380 | 1 | 105 | 500 d | 0.5 | 140 |
| | | | | 500 d | 1.0 | 700 |
| | | | | 500 d | 1.0 | 3200 |
| | | | | 1500 d | 1.0 | 60000 |

an estimation. From the R_g^6 dependence of τ_{syn} in Eq. 1, one can expect large uncertainties in the synchronization timescale as a result of the uncertainties in the red giant radius. There is also a P_{orb}^4 dependence, which can introduce large uncertainties, but P_{orb} is much more accurately known than R_g .

As can be seen in Table 3, for S-type SSs depending on the binary parameters, τ_{syn} can be as short as $< 10^4$ yr and longer than 10^7 years. Short τ_{syn} can be expected when the radius of the mass donor is a significant fraction of the orbital separation.

The lifetime of the symbiotic phase for a red giant or AGB star is around 10^5 year (see e.g. Yungleson et al. 1995), which is comparable with τ_{syn} .

4.2 Inclination

In our calculations, we assume that the rotational axis of the red giant is perpendicular to the orbital plane (see Fekel 1981; Hale 1994; Stawikowski 1994). To calculate the rotational periods of the mass donors (P_{rot}) we need to know the inclination of the orbit (i) and R_g .

For eclipsing binaries we can adopt inclination $i = 70^\circ - 110^\circ$, which produces small errors in $\sin i$. For such cases we will assume that $\sin i$ is in the range 0.94-1.00. For other cases we use results from spectropolarimetric observations or radial velocity measurements.

4.3 Radius of the cool component

For a few objects, the radii of the cool components are derived from model calculations. If the radius of the giant (R_g) is not known, we will use the average radius for the corresponding spectral type taken from van Belle et al.(1999), always adopting luminosity class III and error $\pm 5\%$.

For the M giants these values are similar to the stellar radii of M giants in the Hipparcos catalogue as calculated by Dumm & Schild (1998). Dumm & Schild (1998) have also shown that the radius of the M giants depends on the mass. For 9 objects included in our sample, the masses of the M giants are listed in Mikolajewska(2003). In Table 4, we compare the values adopted here (following van Belle et al. 1999) with the results of Dumm & Schild (1998).

As visible in most cases, the adopted radii (following

Table 4. Stellar radii of M giants. In column 3 are given R_g (following van Belle et al. 1999), in column 4 - mass of the M giants (from Mikołajewska 2003), in column 5 - the range of R_g for the corresponding mass and spectral type (following Dumm & Schild 1998).

| Object | Mass donor | R_g [R_\odot] | M_g [M_\odot] | R_g [R_\odot] |
|--------|------------|------------------------|------------------------|------------------------|
| 1 | 2 | 3 | 4 | 5 |
| FG Ser | M5III | 140 | 1.7 | 110-150 |
| AR Pav | M5III | 140 | 2.5 | 90-240 |
| AG Peg | M3III | 72 | >1.8 | 60-90 |
| BX Mon | M5III | 140 | 3-3.7 | 150-200 |
| SY Mus | M5III | 140 | 1.3 | 60-100 |
| RW Hya | M2III | 58 | 1.6 | 40-80 |
| AR Pav | M5III | 140 | 2.5-3 | 130-160 |
| BF Cyg | M5III | 140 | 1.8 | 110-140 |
| AG Peg | M3III | 72 | \gtrsim 1.8 | 60-90 |

van Belle et al. 1999) are in agreement with the mass-dependent radii of Dumm & Schild (1998). There are 2 cases where the adopted values are outside of this range: BX Mon and SY Mus (see Sect.6).

5 RESULTS

Our measurements of $v \sin i$ together with data collected from the literature, are summarized in Table 2. Our sample thus contains 39 objects (29 with $v \sin i$ measured by us and 10 taken from the literature). This sample should have no biases in the rotational speed of the cool giant, even though the sample is flux limited.

In our sample of S-type SSs, the projected rotational velocities of the mass donors are from 3.5 km s^{-1} up to 52 km s^{-1} . Including our data and the data from the literature, we obtain for $v \sin i$: mean= 8.7 km s^{-1} , median= 7.7 km s^{-1} , standard deviation= 7.4 km s^{-1} .

If we exclude the 2 slowest and the 2 fastest rotators we get: mean $v \sin i = 7.6 \pm 1.8 \text{ km s}^{-1}$. In effect, 90% of the mass donors in S-type SSs with measured rotation have $v \sin i$ in the interval $4.5 \leq v \sin i \leq 11.7 \text{ km s}^{-1}$. For the southern S-type symbiotics (29 objects, flux limited sample, FEROS observations) the values are similar: median $v \sin i = 8.1 \text{ km s}^{-1}$, 90% of the objects in the interval $4 \leq v \sin i \leq 11.7 \text{ km s}^{-1}$.

6 S-TYPE SYMBIOTICS WITH KNOWN ORBITAL PERIODS

In our sample, there are 17 objects with known orbital periods and 1 where this is inferred (V2756 Sgr). In this section we compare the orbital periods with the rotational periods of the mass donors object by object. The upper-lower limits of P_{rot} are calculated from:

$$P_{rot} = \frac{2\pi(R_g \pm e_1)(\sin i \pm e_2)}{v \sin i \mp e_3}, \quad (3)$$

where e_1 , e_2 , and e_3 are the corresponding errors in R_g , $\sin i$, and $v \sin i$ respectively.

In the statistical analysis (Sect.8), for P_{rot} we will use the average value between these upper-lower limits and will consider them as corresponding to $\pm 1\sigma$ error.

6.1 Objects with known orbital periods observed by us

AR Pav is an eclipsing binary with $P_{orb} \approx 604.5$ days (Bruch et al. 1994). The giant's radius derived from the eclipse is $R_g = 137 \pm 20 R_\odot$ (Quiroga et al. 2002), which is very close to the value adopted in Table 2 from the spectral type of the cool giant and to $R_g = 139 \pm 10 R_\odot$ (Skopal 2005). We calculate $649 < P_{rot} < 1120$ days.

AS 289 (V343 Ser) has orbital period $P_{orb} = 450.5 \pm 2.2$ d, $e = 0.135 \pm 0.046$, and orbital inclination of $17^\circ - 23^\circ$ (Fekel et al. 2001). Kenyon & Fernandez-Castro (1987) gave spectral type M3.9III, but more recently M3.5 is assigned from Mürset & Schmid (1999). Assuming it is a normal M3.5III star, and using our CCF value for $v \sin i$, we obtain $159 < P_{rot} < 341$ days.

In a binary with an eccentric orbit the synchronization is reached at a value of $P_{rot} < P_{orb}$ (pseudosynchronization, see Hut 1981). Following Eq. 42 and Eq. 43 of Hut (1981), in AS 289 the pseudosynchronization is expected at $P_{rot} = 0.90 P_{orb}$.

It is worth noting that Fekel et al.(2003) give a value of $v \sin i = 5.7 \pm 1 \text{ km s}^{-1}$ and our FWHM method give $v \sin i = 9.5 \pm 1 \text{ km s}^{-1}$. An independent measurement of $v \sin i$ with better spectroscopic resolution will be valuable.

BD-21°3873 has $P_{orb} = 281.6 \pm 1.2$ days, $\sin i = 0.87$ (Smith et al. 1997). We derive $147 < P_{rot} < 293$ days. The object is thus synchronized within the measurement errors.

RW Hya is an eclipsing binary with $P_{orb} = 370.4 \pm 0.8$ days (Schild et al. 1996). Supposing $i = 70^\circ - 90^\circ$, we calculate that P_{rot} is in the interval 301 - 552 days. The object is thus synchronized within the measurement errors.

FG Ser (AS 296) is an eclipsing binary with $P_{orb} = 650 \pm 5$ days (Mürset et al. 2000). Supposing $i = 70^\circ - 90^\circ$, we calculate $P_{rot} \approx 563 - 918$ days. The object is thus synchronized within the measurement errors.

6.2 Objects with known periods, not observed by us

Fekel, Hinkle & Joyce (2004) published values of $v \sin i$ for 13 S-type SSs. In this section, if not otherwise stated, we use their measurements.

SY Mus is an eclipsing binary with $i = 95^\circ.8 \pm 1.7^\circ$ (Harries & Howarth 1996, 2000), $P_{orb} = 624.5$ days and $v \sin i = 7 \pm 1 \text{ km s}^{-1}$ (Pereira et al.1995; Schmutz et al. 1994; Kenyon & Mikołajewska 1995). We calculate $P_{rot} \approx 830 - 1230$ days. [If we use $R_g \approx 80 R_\odot$ (see Sect.4.3), we get $P_{rot} \approx 480 - 705$ days, a range which includes the orbital period.]

AG Dra is a yellow SS with spectroscopic $P_{orb} = 548.5 \pm 2$ d (Friedjung et al. 2003; Fekel et al. 2000b), and $i \approx 30^\circ - 45^\circ$ (Mikołajewska et al.1995). The cool component is a K2 Ib or II (Zhu et al. 1999). There are two measurements of $v \sin i$: $5.9 \pm 1.0 \text{ km s}^{-1}$ (de Medeiros & Mayor 1999) and $3.6 \pm 1.0 \text{ km s}^{-1}$ (Fekel et al. 2004). We adopt $v \sin i = 4.8 \pm 1.0 \text{ km s}^{-1}$. Skopal (2005) calculated

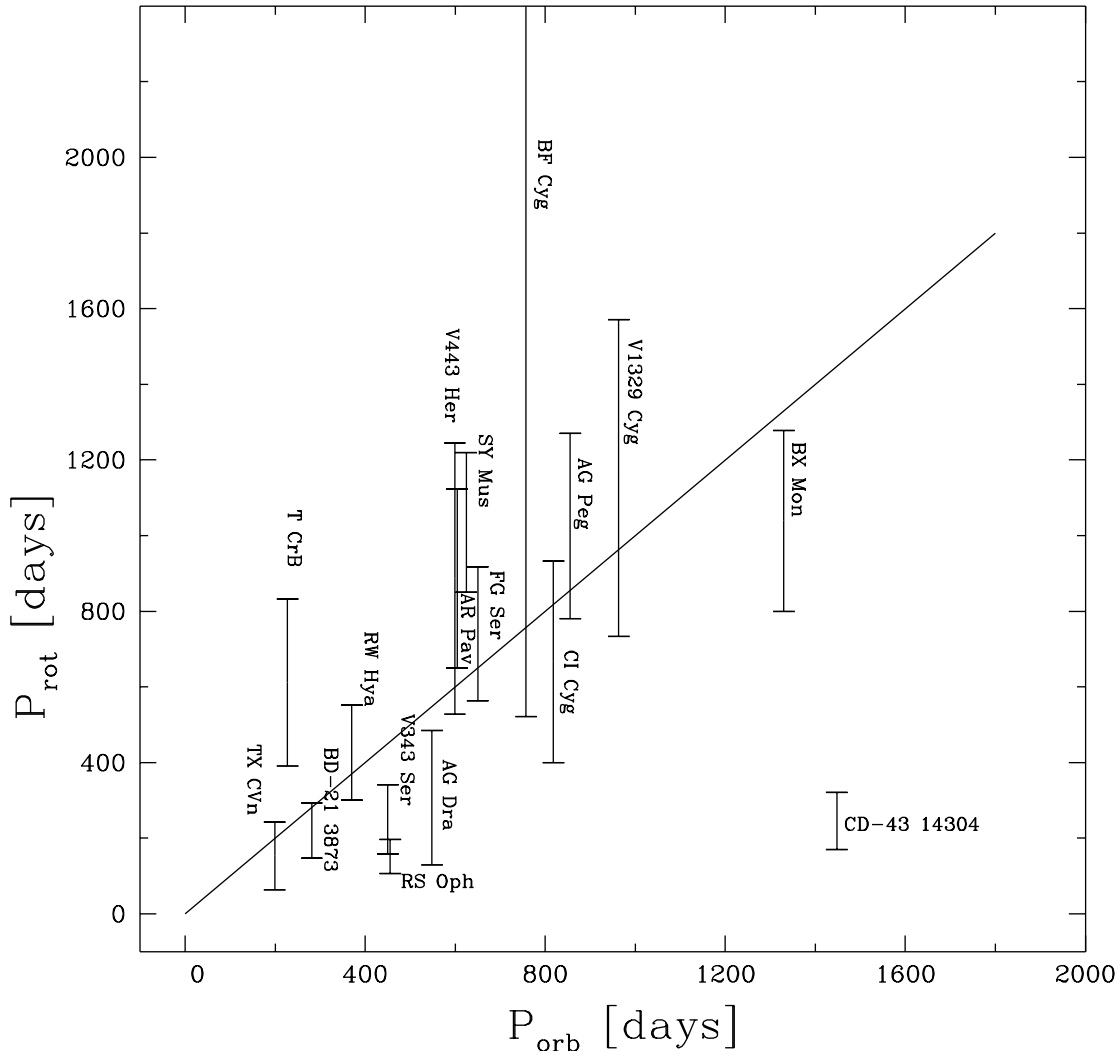


Figure 2. The rotational period of the red giant (P_{rot}) versus the orbital period (P_{orb}) of the 17 objects in our sample. The solid line corresponds to $P_{rot} = P_{orb}$. Most objects are close to this line, which indicates that they are synchronized. There are 2 objects which deviate considerably from that rule (RS Oph and CD-43°14304).

$R_g = 33 \pm 11 R_\odot$. Following Tomov et al.(2000) and the references therein we can adopt $R_g = 30 - 40 R_\odot$. We then estimate $P_{rot} \approx 130 - 485$ days.

TX CVn has $P_{orb} = 199 \pm 3$ d, $e = 0.16 \pm 0.06$, with the cool component a normal K5III star, and inclination $20^\circ < i < 70^\circ$ (Kenyon & Garcia 1989). The luminosity class could also be II or Ib (Zhu et al. 1999). We calculate $P_{rot} \approx 64 - 242$ days. Pseudosynchronization (see Hut 1981) is expected at $P_{rot} = 0.87P_{orb}$. The object is thus (pseudo)synchronized within the measurement errors.

AG Peg has $P_{orb} = 818.2 \pm 1.6$ days and $e = 0.110 \pm 0.039$ (Fekel et al. 2000a), normal M3III and $i \sim 40^\circ - 60^\circ$ (Kenyon et al. 1993). We calculate $P_{rot} \approx 400 - 933$ days. The object is thus synchronized within the measurement errors.

V1329 Cyg has $P_{orb} = 963.1 \pm 9.8$ days (Chochol & Wilson 2001) and inclination $i = 86^\circ \pm 2^\circ$ (Schild & Schmid

1997). We calculate $P_{rot} \approx 734 - 1571$ days. The object is thus synchronized within the measurement errors.

T CrB has $P_{orb} = 227.57$ d (Fekel et al. 2000a), and $R_g = 66 \pm 11 R_\odot$ (Belczynski & Mikolajewska 1998). [It should be noted that Skopal (2005) gives $R_g = 75 \pm 12(d/960pc)$, and that a normal M4III would have $R_g \approx 105.5R_\odot$.] The inclination of the system is $i \approx 65^\circ - 70^\circ$ (Stanishev et al. 2004).

We calculate $P_{rot} \approx 391 - 832$ days, which differs from the expectations for synchronization. This result is unexpected, however it appears that this deviation is not statistically significant (see Table 5). From Eq.1 we get $\tau_{syn} < 100$ yr. The red giant in T CrB is ellipsoidally shaped (Yudin & Munari 1993). This means that the object has to be synchronized.

BX Mon The orbital parameters of this eclipsing system are: $P_{orb} = 1401$ days, eccentricity $e = 0.49$ (Dumm et al. 1998);

$P_{orb} = 1259$ d, $e = 0.44$ (Fekel et al. 2000a).

We calculate $P_{rot} \approx 800 - 1278$ days [if we use $R_g \approx 170 R_\odot$ (see Sect.4.3), we get $P_{rot} \approx 970 - 1550$ days]. BX Mon is the only SS with considerable orbital eccentricity in our sample. SSs with $P_{orb} > 800$ days tends to eccentric orbits (Fekel et al. 2007). In a binary with $e = 0.44$, the pseudosynchronization is expected at about $P_{rot} = 0.46 P_{orb}$ (see Hut 1981).

The time scale for synchronization in SSs is ~ 10 times shorter than the circularization time (see Schmutz et al. 1994). All this implies that in this system the red giant is more or less (pseudo)synchronized, but the orbit is not circularized yet. It has therefore to be in the process of circularization.

V443 Her is not eclipsing, with $P_{orb} = 599.4 \pm 2.1$ days (Fekel et al. 2000b), viewed at an inclination $i \sim 30^\circ$ (Dobrzycka et al. 1993). We calculate $P_{rot} = 528 - 1245$ days. The red giant is thus synchronized within the measurement errors.

CI Cyg is an eclipsing binary with orbital period 855.6 days and orbital separation $a = 2.2$ au (Kenyon et al. 1995). Kenyon et al.(1995) have shown that the mass donor is an M5II asymptotic branch giant, filling its tidal surface. They calculated from the eclipse that $R_g/a \sim 0.4 - 0.5$ which means that $R_g \approx 189 - 236 R_\odot$. We calculate $P_{rot} = 780 - 1270$ days. The object is thus synchronized within the measurement errors.

BF Cyg is an eclipsing binary with $P_{orb} = 757.3$ days and inclination $i \approx 70 - 90^\circ$ (Pucinkas 1970, Skopal et al. 1997). If the cool component is a normal M5III giant we expect $R_g = 139.6 \pm 5\% R_\odot$. Mikolajewska et al.(1989) suggested $R_g \sim 75 R_\odot$, however Skopal et al. (1997) give $R_g = 260 \pm 20 R_\odot$. Using $v \sin i = 4.5 \pm 2 \text{ km s}^{-1}$, we calculate $P_{rot} \sim 560 - 5660$ days.

There are signs that the red giant is ellipsoidally shaped (Yudin et al. 2005). τ_{syn} for such an object will be short, from Eq.1 we get $\tau_{syn} < 7000$ yr. It means that the red giant has to be tidally locked and most probably the R_g is closer to a value $\sim 75 R_\odot$.

7 QUESTIONABLE OBJECTS

RS Oph has orbital period $P_{orb} = 455.72 \pm 0.83$ days (Fekel et al. 2000a). The inclination is about $30 - 40^\circ$ (Dobrzycka & Kenyon 1994; Dobrzycka et al. 1996). This will give a $108 < P_{rot} < 197$ days, i.e. 2-3 times less than the orbital period.

RS Oph is a peculiar SS exhibiting different types of activity – recurrent nova eruptions, jet or blob ejections, flickering (see Bode et al. 2006 and references therein).

This is one of the two objects in our sample whose deviation from synchronization is statistically significant (at confidence level $> 99\%$, see Table 5). The red giant in RS Oph seems to rotate faster than the orbital period, which means that it has to be in a process of deceleration (the expected $\tau_{syn} \leq 5.10^4$ yr).

While there are no doubts about P_{orb} , any of the other parameters ($v \sin i$, inclination, red giant radius) have to be checked with independent measurements.

It is noteworthy that our experiments to measure $v \sin i$

with CCF and spectra from different epochs showed that $v \sin i$ could even be higher (up to $14.5 \pm 1.5 \text{ km s}^{-1}$).

CD-43°14304 Schmid et al.(1998) reported a circular orbit, $P_{orb} = 1448 \pm 100$ days. They argued that the presence of phase-dependent $H\alpha$ variations is attributable to occultation effects, suggesting a relatively high inclination, $i > 45^\circ$. Spectropolarimetry (Harries & Howarth 2000) gives two possible values for the inclination of the system $i = 57^\circ \pm 5^\circ$ or $i = 122^\circ \pm 48^\circ$. The second corresponds to an improbably large eccentricity for the orbit. Therefore we can accept $\sin i = 0.79 - 0.88$. With our value of $v \sin i$ we calculate $P_{rot} \approx 170 - 321$ days.

However, Schmid et al.(1998) found no evidence for rotational broadening in the cool-giant spectrum and were able to place an upper limit on $v \sin i < 3 \text{ km s}^{-1}$. We measured $v \sin i = 7.2 \pm 1.5 \text{ km s}^{-1}$ the CCF looks good (see Fig. 5) and FWHM method gives a similar result. If our CCF result is wrong and that of Schmid et al.(1998) is a correct one, then the object is probably synchronized. To avoid confusion we will exclude this star from the analysis, but an independent check of $v \sin i$ would be valuable.

V2756 Sgr (Hen 2-370, SS73 145). The parameters of the system are not well known. We calculate $P_{rot} < 1595$ days. A photometric period of 243 days is supposed in Hoffleit (1970). This photometric period is not confirmed with radial velocity measurements to be that of the orbit. If this is the orbital period and the red giant is tidally locked, then the inclination of the system would be about $i \sim 15^\circ$.

Hen 3-1674 is the fastest rotator in our sample. The catalogues indicate that the mass donor is probably M5III star (see Table 2 and the references therein). A normal M5III star would have $R_g \approx 90 - 160 R_\odot$ (van Belle et al 1999) and $M_g \approx 1 - 3 M_\odot$, which means a break-up velocity of 30-60 km s^{-1} . If our measurements and the adopted parameters of the system are correct then Hen 3-1674 rotates close to its critical velocity and has rotation similar to that of D'-type SSs (see Paper I).

8 ARE THE MASS DONORS IN S-TYPE SYMBIOTICS SYNCHRONIZED (CO-ROTATING) ?

Fig. 2 shows the rotational period versus the orbital period of the 17 objects in our sample, with a straight line indicating the co-rotation (i.e. $P_{rot} = P_{orb}$). Most objects are close to this line, which suggests that they are synchronized. In Table 5 are given the individual deviations as well as the corresponding probability that the deviation is random. 9 objects are synchronized within the measurement errors ($1-\sigma$ level). 4 objects have deviations between 1 and $2-\sigma$. Generally, 15 out of 17 are within the $3-\sigma$ level. The two objects that are outside of the $3-\sigma$ level are RS Oph and CD-43°14304.

The standard χ^2 test gives a probability of $p(\chi^2) < 10^{-6}$ that the co-rotation straight line fits the data points when we use all 17 objects. Here we have considered the errors of the rotational period only, the errors of P_{orb} are supposed to be small (usually they are $< 2\%$). The straight line cannot be rejected as a fit to the data at more than 90% confidence level, $p(\chi^2) = 0.127$, when the two deviating objects (CD-43°14304 and RS Oph) are excluded. The χ^2 statistic tests how well the data are described by the model,

assuming that all the deviations are due to measurement errors and not to intrinsic scatter.

When intrinsic scatter is allowed, as we expect to be the more realistic situation, one can apply the weighted least squares estimator (e.g. Akritas & Bershad 1996) to find the slope (β) and the intercept (α) of a linear fit in the form $P_{rot} = \alpha + \beta P_{orb}$ to the data points with measurement errors and non-negligible intrinsic scatter. When all objects are included, we get $\alpha = 204 \pm 49$ and $\beta = 0.14 \pm 0.07$, which is not consistent with $P_{rot} = P_{orb}$ ($\alpha = 0, \beta = 1.0$). The situation changes if CD-43°14304 is removed from the sample, then $\alpha = -110 \pm 77$ and $\beta = 0.93 \pm 0.16$. When the deviating recurrent nova RS Oph is removed as well, we obtain $\alpha = -32 \pm 78$ and $\beta = 1.01 \pm 0.17$. The last result is fully consistent with $P_{orb} = P_{rot}$ line ($\alpha = 0, \beta = 1$).

Although the synchronization line seems to fit well the data, we still cannot rule out the possibility that one or more outlying objects may determine a false correlation between the variables. Therefore, a rank correlation test appears appropriate. The Spearman rank correlation coefficient between the two periods is 0.61 when all 17 objects were included, and about 0.82 for 16 and 15 objects only. This result implies a significant correlation between the variables, since the p-values are less than 0.02 and 0.002 respectively. The similar Kendall-tau test gives similar results, with p-values less than 0.01 for all cases.

The objects that deviate significantly from the $P_{orb} = P_{rot}$ line are RS Oph (a peculiar SS as noted above) and CD-43°14304 (with possible error in the $v \sin i$ measurement, see Sect.7). Taking into account the uncertainties of their P_{rot} , one finds that the probabilities for a random deviation are less than 0.01 for them (see Table 5), while for all the other 15 stars this idea cannot be rejected at the 0.01 significance level. In other words the null hypothesis that all S-type SSs with well measured $v \sin i$ are synchronized (excluding RS Oph and CD-43°14304) cannot be rejected at the 99% confidence level.

An additional test that may give some clues about the extent of synchronization of the periods is the K-S test of how much $(P_{rot} - P_{orb})/\sigma$ deviates from the normal distribution. Even when all 17 stars are included, the p-value of the K-S statistics is slightly less than 10%. When only the above 15 objects are included (see Fig.3), the distribution becomes much narrower (mean = 0.15, $\sigma = 1.23$, K-S statistics is 0.38), with a standard deviation comparable to the measurement errors of P_{rot} , $\langle \sigma/P_{rot} \rangle = 0.53$. This means that the hypothesis that the sample comes from a normal distribution cannot be rejected statistically.

We see that the null hypothesis for synchronization of the red giants in symbiotic stars cannot be rejected statistically (except probably for RS Oph).

9 CLUES TO THE ORBITAL PERIODS

Up to now, out of 188 SSs, the orbital elements and binary periods are well known for ~ 40 objects only (and they are all S-type). The derived orbital periods are in the range 200 – 2000 days (Mikołajewska 2003).

Because the orbital periods of the majority of SSs are unknown, an indirect method to obtain P_{orb} is to measure $v \sin i$. If the mass donors in SSs are co-rotating

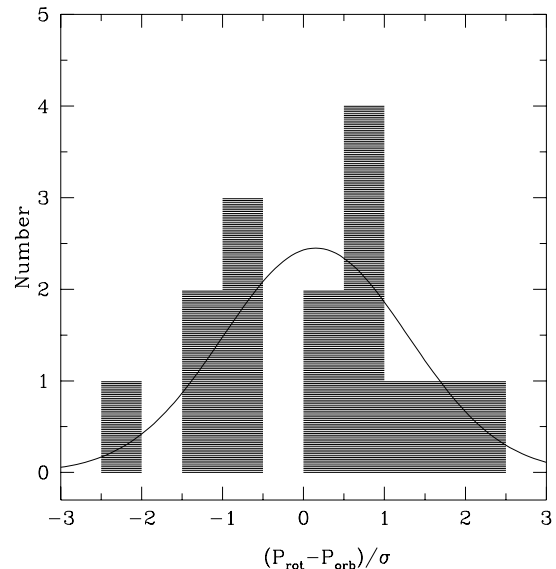


Figure 3. The distribution of $(P_{rot} - P_{orb})/\sigma$ for 15 symbiotic stars and the fitted gaussian (σ is the error of P_{rot}). The K-S statistic gives only a 38% probability that the parent distribution deviates from the normal one (not statistically significant).

Table 5. The deviations of the individual objects from the line $P_{rot} = P_{orb}$. In the second column the deviations are given in units of σ , where σ is the individual error of P_{rot} . The third column gives the probability for random deviation. To reject the null hypothesis (synchronization) at 99% confidence level, $p(\chi^2)$ has to be smaller than 0.01.

| Object | deviation [σ] | $p(\chi^2)$ |
|-------------|---------------------------|-------------|
| SY Mus | 2.2 | 0.026 |
| AG Dra | 1.4 | 0.175 |
| BX Mon | 1.2 | 0.223 |
| TX CVn | 0.5 | 0.605 |
| T CrB | 1.7 | 0.082 |
| V443 Her | 0.8 | 0.423 |
| CI Cyg | 0.7 | 0.489 |
| AG Peg | 0.6 | 0.569 |
| V1329 Cyg | 0.5 | 0.651 |
| BF Cyg | 0.9 | 0.361 |
| AR Pav | 1.2 | 0.233 |
| V343 Ser | 2.2 | 0.028 |
| BD-21°3873 | 0.8 | 0.399 |
| CD-43°14304 | 15.9 | $< 10^{-6}$ |
| FG Ser | 0.5 | 0.610 |
| RS Oph | 6.7 | $< 10^{-6}$ |
| RW Hya | 0.4 | 0.655 |

$(P_{rot} = P_{orb})$, we can find clues for the orbital periods via the simple relation $P_{orb} v_{rot} = 2\pi R_g$, where P_{orb} is the orbital period, v_{rot} and R_g are the rotational velocity and radius of the giant, respectively. The underlying suppositions are: **(1)** corotation (see Sect. 8) and **(2)** rotational axis of the red giant perpendicular to the orbital plane (see Sect. 4.2 and references therein).

It could be useful in the case of eclipsing binaries, where $\sin i \approx 1$ and $v \sin i \approx v_{rot}$, however in such cases it is easy to find P_{orb} with photometry. If the inclination is

unknown, we can only put an upper limit, $P_{orb} \lesssim P_{ul}$, where $P_{ul} = 2\pi R_g/v \sin i$. To see how useful this predictor is, we calculated the upper limits for the objects with known orbital periods, and we get $P_{ul}/P_{orb} \sim 0.5 - 1.5$.

For the objects with unknown periods, the upper limits for P_{orb} calculated in this way are given in the last column of Table 2. These upper limits are in the interval 100–1500 days. Most of them are similar to those of the measured orbital periods in S-type SSs. However, it seems that for AS 255 and Hen 3-1674, P_{orb} could be as short as $\lesssim 150$ days.

10 CONCLUSIONS

We have observed 30 S-type symbiotic stars with the FEROS spectrograph. We have measured the rotational velocities of the mass donors for 29 of them by the means of the CCF method (for V3804 Sgr we did not get a meaningful CCF). The results of the CCF method have been checked by the FWHM measurements. The main results are:

(1) The projected, rotational velocities of the cool components in S-type symbiotic stars are from 3.5 km s^{-1} up to 52 km s^{-1} and 90% of them are in the interval from 4.5 km s^{-1} to 11.7 km s^{-1} .

(2) In our sample of 17 S-type SSs with known orbital periods, 9 are synchronized within the measurement errors ($1-\sigma$ level). If we exclude the doubtful object CD-43°14304 and the recurrent nova RS Oph, **all remaining 15 objects are synchronized within the $3-\sigma$ level**. In other words, the null hypothesis that these 15 objects are synchronized can not be rejected statistically at the 99% confidence level.

(3) Among all objects with $v \sin i$ measured by us the deviation from synchronization is statistically significant (at the 99% confidence level) only for RS Oph. The red giant in this peculiar object seems to rotate faster than the orbital period.

(4) For 22 S-type SSs with unknown parameters, we give clues as to what their orbital periods could be.

In future it will be interesting: (i) to measure the projected rotational velocity of the cool giants in more symbiotic stars; (ii) to compare their rotational velocity with that of the isolated giants and those in other binary systems.

ACKNOWLEDGMENTS

This research has made use of SIMBAD, IRAF, and Starlink. RZ was supported by a PPARC Research Assistantship and MFB was a PPARC Senior Fellow. AG acknowledges the receipt of Marie Curie Fellowship and Marie Curie European Re-integration Grant from the European Commission. This work was partially complete when Dr John Porter passed away in June 2005 and we dedicate this paper to his memory.

REFERENCES

Allen, D. A. 1982, *ASSL Vol. 95: IAU Colloq. 70: The Nature of Symbiotic Stars*, 27
 Akritas, M. G., & Bershad, M. A. 1996, *ApJ*, 470, 706
 Baranne, A., Mayor, M., & Poncet, J. L. 1979, *Vistas in Astronomy*, 23, 279
 Belczyński, K., & Mikolajewska, J. 1998, *MNRAS*, 296, 77

Belczyński, K., Mikolajewska, J., Munari, U., Ivison, R. J., & Friedjung, M., 2000, *A&AS*, 146, 407
 Bode, M. F., O'Brien, T. J., Osborne, J. P., et al. 2006, *ApJ*, 652, 629
 Bruch, A., Niehues, M., & Jones, A. F. 1994, *A&A*, 287, 829
 Chochol, D., & Wilson, R. E. 2001, *MNRAS*, 326, 437
 Corradi, R. L. M., Mikolajewska, J., & Mahoney, T. J. 2003, *Symbiotic Stars Probing Stellar Evolution*, *Astronomical Society of the Pacific Conference Series*, 303
 de Medeiros, J. R., & Mayor, M. 1999, *A&AS*, 139, 433
 Delfosse, X., Forveille, T., Perrier, C., & Mayor, M. 1998, *A&A*, 331, 581
 Dobrzycka, D., & Kenyon, S. J. 1994, *AJ*, 108, 2259
 Dobrzycka, D., Kenyon, S. J., Proga, D., Mikolajewska, J., & Wade, R. A. 1996, *AJ*, 111, 2090
 Dumm, T., Muerset, U., Nussbaumer, H., Schild, H., Schmid, H. M., Schmutz, W., & Shore, S. N. 1998, *A&A*, 336, 637
 Dumm, T., & Schild, H. 1998, *New Astronomy*, 3, 137
 Fekel, F. C., Jr. 1981, *ApJ*, 246, 879
 Fekel, F. C. 1997, *PASP*, 109, 514
 Fekel, F. C., Joyce, R. R., Hinkle, K. H., & Skrutskie, M. F. 2000a, *AJ*, 119, 1375
 Fekel, F. C., Hinkle, K. H., Joyce, R. R., & Skrutskie, M. F. 2000b, *AJ*, 120, 3255
 Fekel, F. C., Hinkle, K. H., Joyce, R. R., & Skrutskie, M. F. 2001, *AJ*, 121, 2219
 Friedjung, M., Gális, R., Hric, L., & Petrik, K. 2003, *A&A*, 400, 595
 Fekel, F. C., Hinkle, K. H., & Joyce, R. R. 2004, *IAU Symposium*, 215, 168
 Fekel, F. C., Hinkle, K. H., Joyce, R. R., Wood, P. R., & Lebzelter, T. 2007, *AJ*, 133, 17
 Gray, D. F. 1976, *The observation and analysis of stellar photospheres*, Research supported by the National Research Council of Canada. New York, Wiley-Interscience, 1976. 484 p.
 Hale, A. 1994, *AJ*, 107, 306
 Harries, T. J., & Howarth, I. D. 1996, *A&A*, 310, 235
 Harries, T. J., & Howarth, I. D. 2000, *A&A*, 361, 139
 Henry, G. W., Fekel, F. C., Henry, S. M., & Hall, D. S. 2000, *ApJS*, 130, 201
 Hoffleit, D. 1970, *Informational Bulletin on Variable Stars*, 469, 1
 Hubeny I., Lanz T., Jeffery C.S., 1994, in Jeffery C.S., eds, *Newsletter on Analysis of Astronomical Spectra*, No.20, CCP7 St. Andrews Univ., St. Andrews, p.30
 Hut, P. 1981, *A&A*, 99, 126
 Kaufer, A., Stahl, O., Tubbesing, S., Norregaard, P., Avila, G., Francois, P., Pasquini, L., & Pizzella, A. 1999, *The Messenger*, 95, 8
 Kenyon, S. J. 1986, *The symbiotic stars*, Cambridge and New York, Cambridge University Press, 1986, 295 p.,
 Kenyon, S. J., & Fernandez-Castro, T. 1987, *AJ*, 93, 938
 Kenyon, S. J., & Garcia, M. R. 1989, *AJ*, 97, 194
 Kenyon, S. J., & Mikolajewska, J. 1995, *AJ*, 110, 391
 Keyes, C. D., & Preblich, B. 2004, *AJ*, 128, 2981
 Kenyon, S. J., Mikolajewska, J., Mikolajewski, M., Polidan, R. S., & Slovak, M. H. 1993, *AJ*, 106, 1573
 Kupka F., Piskunov N.E., Ryabchikova TA., Stempels H.C., Weiss W.W., 1999, *A&AS*, 138, 119

Kurucz R.L., 1993, ATLAS9 Stellar Atmosphere Programs (Kurucz CD-ROM 13)

Medina Tanco, G. A., & Steiner, J. E. 1995, *AJ*, 109, 1770

Melo, C. H. F., Pasquini, L., & De Medeiros, J. R. 2001, *A&A*, 375, 851

Melo, C. H. F. 2003, *A&A*, 410, 269

Mikolajewska, J., Mikolajewski, M., & Kenyon, S. J. 1989, *AJ*, 98, 1427

Mikolajewska, J., Kenyon, S. J., Mikolajewski, M., Garcia, M. R., & Polidan, R. S. 1995, *AJ*, 109, 1289

Mikolajewska, J. 2003, *Astronomical Society of the Pacific Conference Series*, 303, 9

Mürset, U., & Schmid, H. M. 1999, *A&AS*, 137, 473

Mürset, U., Dumm, T., Isenegger, S., Nussbaumer, H., Schild, H., Schmid, H. M., & Schmutz, W. 2000, *A&A*, 353, 952

Nordström, B., et al. 2004, *A&A*, 418, 989

Pereira, C. B., Vogel, M., & Nussbaumer, H. 1995, *A&A*, 293, 783

Pereira, C. B., Smith, V. V., & Cunha, K. 2005, *A&A*, 429, 993

Pucinskas, A. 1970, *Vilnius Astronomijos Observatorijos Biuletėnis*, 27, 24

Quiroga, C., Mikolajewska, J., Brandi, E., Ferrer, O., & García, L. 2002, *A&A*, 387, 139

Schild, H., Muerstet, U., & Schmutz, W. 1996, *A&A*, 306, 477

Schild, H., Dumm, T., Mürset, U., Nussbaumer, H., Schmid, H. M., & Schmutz, W. 2001, *A&A*, 366, 972

Schmid, H. M., Dumm, T., Mürset, U., Nussbaumer, H., Schild, H., & Schmutz, W. 1998, *A&A*, 329, 986

Schmidt-Kaler, T. H. 1982, in *Landolt-Brnstein, New Series, Group VI, Vol. 2b, Stars and Star Clusters*, ed. K. Schaifers & H. H. Voigt (New York: Springer)

Schmutz, W., Schild, H., Muerstet, U., & Schmid, H. M. 1994, *A&A*, 288, 819

Skopal, A., Vittone, A., Errico, L., Bode, M. F., Lloyd, H. M., & Tamura, S. 1997, *MNRAS*, 292, 703

Skopal, A. 2005, *A&A*, 440, 995

Smith, V. V., Cunha, K., Jorissen, A., & Boffin, H. M. J. 1997, *A&A*, 324, 97

Smith, V. V., Pereira, C. B., & Cunha, K. 2001, *ApJ*, 556, L55

Soker, N. 2002, *MNRAS*, 337, 1038

Stanishev, V., Zamanov, R., Tomov, N., & Marziani, P. 2004, *A&A*, 415, 609

Stawikowski, A. 1994, *Acta Astronomica*, 44, 393

Tassoul, J. 2000, *Stellar rotation / Jean-Louis Tassoul*. Cambridge ; New York : Cambridge University Press, 2000 (Cambridge astrophysics series 36)

Tomov, N. A., Tomova, M. T., & Ivanova, A. 2000, *A&A*, 364, 557

van Belle, G. T., Lane, B.F., Thompson, R.R., Dodson, A.F., Colavita, M.M., et al. 1999, *AJ*, 117, 521

Yudin, B., & Munari, U. 1993, *A&A*, 270, 165

Yudin, B. F., Shenavrin, V. I., Kolotilov, E. A., Tatarnikova, A. A., & Tatarnikov, A. M. 2005, *Astronomy Reports*, 49, 232

Yungelson, L., Livio, M., Tutukov, A., & Kenyon, S. J. 1995, *ApJ*, 447, 656

Zahn, J.-P. 1977, *A&A*, 57, 383

Zahn, J.-P. 1989, *A&A*, 220, 112

Zamanov, R. K., Bode, M. F., Melo, C. H. F., Porter, J., Gomboc, A., & Konstantinova-Antova, R. 2006, *MNRAS*, 365, 1215 (Paper I)

Zhu, Z. X., Friedjung, M., Zhao, G., Hang, H. R., & Huang, C. C. 1999, *A&AS*, 140, 69

APPENDIX

Here we give a few examples of our spectra (Fig. 4) and graphic representation of the CCF for all SSs observed in this paper (Fig.5).

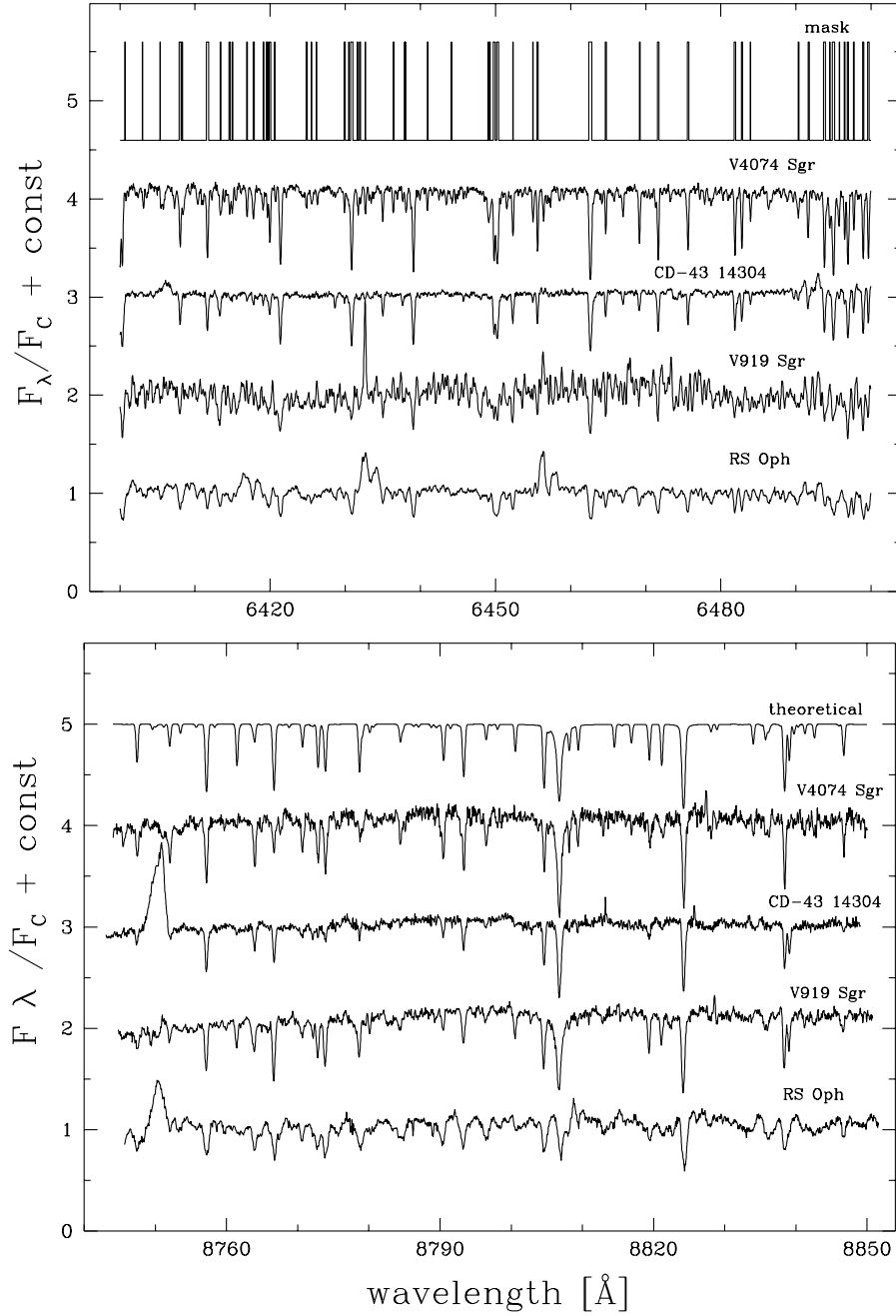


Figure 4. A few examples of our spectra, together with the mask in the interval $\lambda\lambda 6400 - 6500$ Å (upper panel), and with a synthetic spectrum in the interval $\lambda\lambda 8740 - 8850$ Å. The spectra are plotted in increasing order of rotation: V4074 Sgr (M4III, $v \sin i = 3.5 \text{ km s}^{-1}$), CD-43°14304 (K5III, $v \sin i = 7.2 \text{ km s}^{-1}$), V919 Sgr (M2III, $v \sin i = 9.1 \text{ km s}^{-1}$), RS Oph (M0III, $v \sin i = 11.7 \text{ km s}^{-1}$). The synthetic spectrum corresponds to M0III and $v \sin i = 5 \text{ km s}^{-1}$.

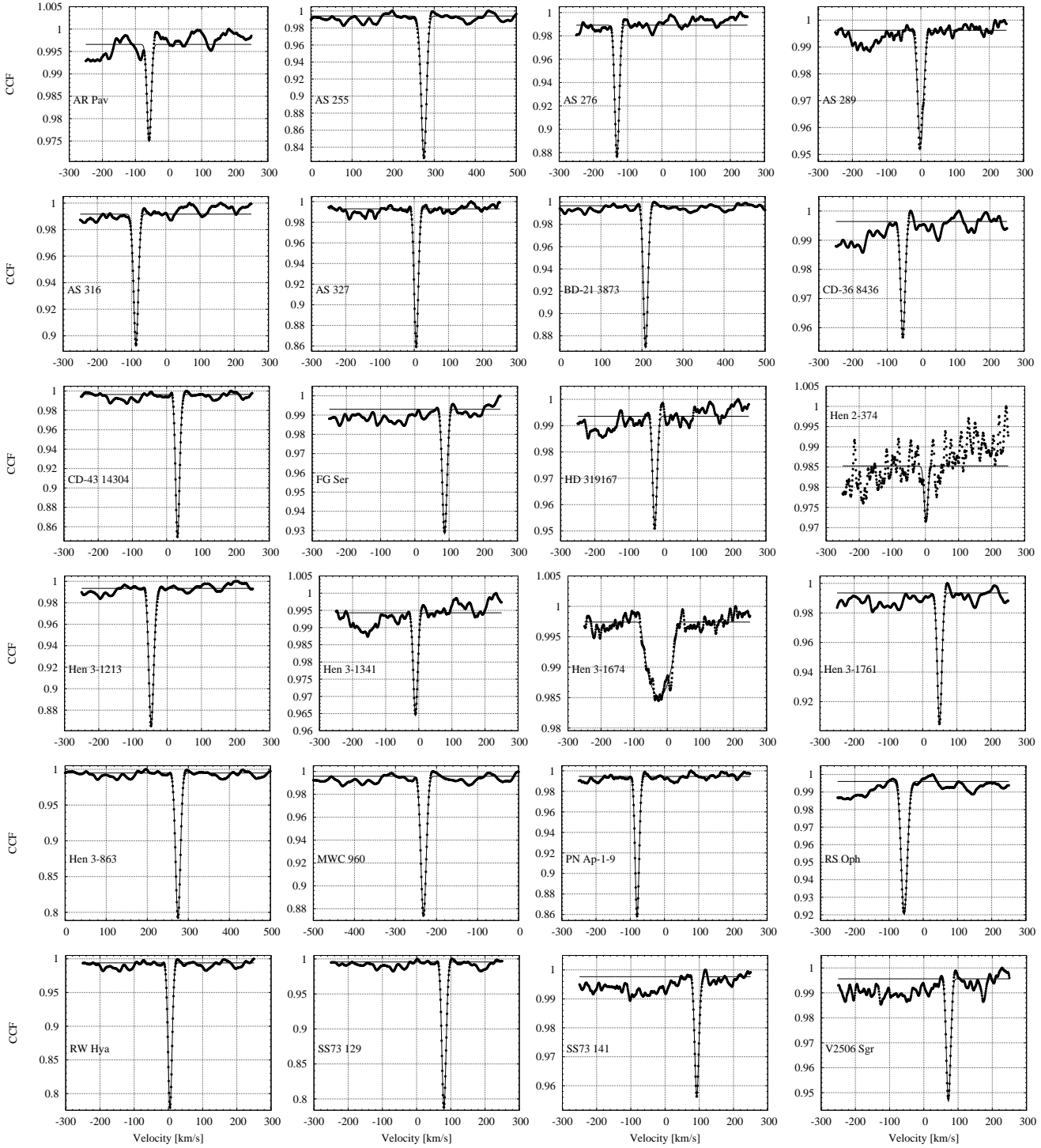


Figure 5. CCF using K0 numerical mask. In each panel are plotted the relative intensity of CCF (heavy line) and the fit versus radial velocity for the SSs observed in this paper. The measured widths of the CCF are given in Table 2.

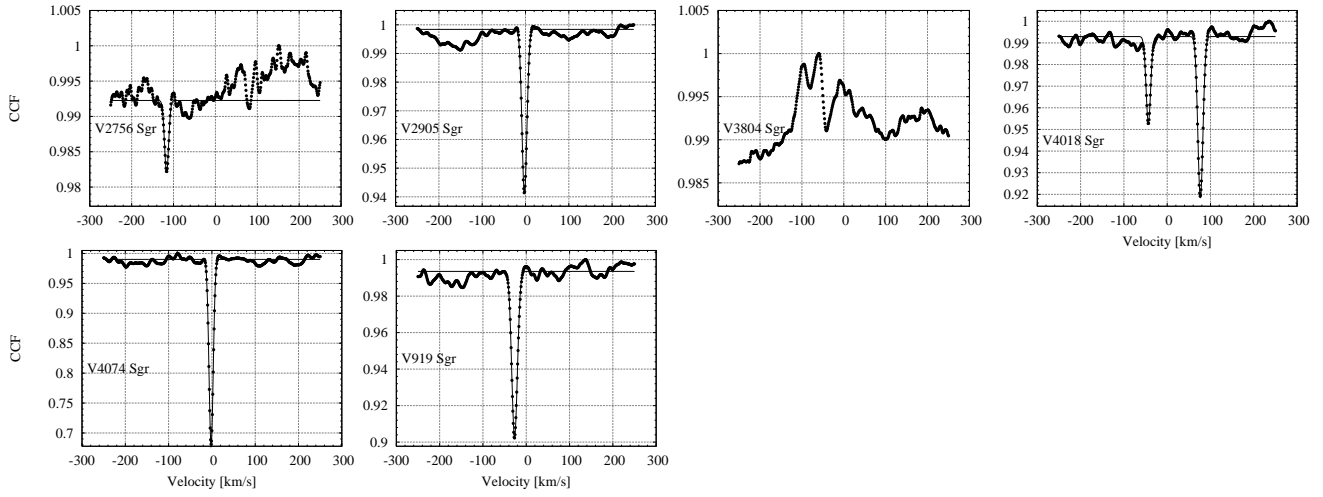


Figure 5. continuation